Biophysical Journal
Article

Biophysical Society

Binding-induced lipid domains: Peptide-membrane interactions with PIP_2 and PS

Ziareena A. Al-Mualem,[1] Xiaobing Chen,[1] Azam Shafieenezhad,[2] Eric N. Senning,[2,*] and Carlos R. Baiz[1,*]
[1]Department of Chemistry, The University of Texas at Austin, Austin, Texas and [2]Department of Neuroscience, The University of Texas at Austin, Austin, Texas

ABSTRACT Cell signaling is an important process involving complex interactions between lipids and proteins. The myristoylated alanine-rich C-kinase substrate (MARCKS) has been established as a key signaling regulator, serving a range of biological roles. Its effector domain (ED), which anchors the protein to the plasma membrane, induces domain formation in membranes containing phosphatidylinositol 4,5-bisphosphate (PIP_2) and phosphatidylserine (PS). The mechanisms governing the MARCKS-ED binding to membranes remain elusive. Here, we investigate the composition-dependent affinity and MARCKS-ED-binding-induced changes in interfacial environments using two-dimensional infrared spectroscopy and fluorescence anisotropy. Both negatively charged lipids facilitate the MARCKS-ED binding to lipid vesicles. Although the hydrogen-bonding structure at the lipid-water interface remains comparable across vesicles with varied lipid compositions, the dynamics of interfacial water show divergent patterns due to specific interactions between lipids and peptides. Our findings also reveal that PIP_2 becomes sequestered by bound peptides, while the distribution of PS exhibits no discernible change upon peptide binding. Interestingly, PIP_2 and PS become colocalized into domains both in the presence and absence of MARCKS-ED. More broadly, this work offers molecular insights into the effects of membrane composition on binding.

SIGNIFICANCE This study explores cell signaling mechanisms by investigating myristoylated alanine-rich C-kinase substrate protein binding to phosphatidylinositol 4,5-bisphosphate and phosphatidylserine lipids. Myristoylated alanine-rich C-kinase substrate binding induces lipid domain separation in plasma membranes, influencing the local environments at the lipid-water interface. These findings shed light on the molecular mechanisms of cell signaling and help obtain a better understanding of lipid-protein interactions during cellular functions. The finding of phosphatidylinositol 4,5-bisphosphate/phosphatidylserine colocalization in signaling pathways is significant because it reveals how lipid species cooperate in shaping cellular responses. Ultimately, this study advances our understanding of signaling, potentially guiding innovative strategies and new therapies that target lipid-protein interactions.

INTRODUCTION

Cell signaling is a complex process facilitated by interactions involving diverse set of biomolecules (1,2). Signaling networks drive cellular processes including differentiation and division or cell-specific functions such as axon regeneration in neurons. The convergence of signaling networks on select proteins has brought several of these to prominence (3,4). The protein myristoylated alanine-rich C-kinase substrate (MARCKS) has been implicated as an important regulator in myriad cell signaling networks and an important component in normal brain development (5–9).

Ongoing studies of MARCKS as a mediator in protein kinase C (PKC)-based phosphorylation focus on the translocation of MARCKS to and from the plasma membrane. A myristoylation site in the N-terminal region of MARCKS is a hydrophobic membrane insertion point for the protein, which promotes interaction of the protein with the plasma membrane (10,11) (Fig. 1). However, the poly-lysine rich effector domain (ED), when expressed as a protein fragment (151–175), is also known to associate with lipid bilayers. Numerous positively charged lysine residues in the MARCKS-ED facilitate association of the entire MARCKS protein with lipid membranes (12). Signaling through MARCKS is achieved through PKC

Submitted September 19, 2023, and accepted for publication December 20, 2023.

*Correspondence: esen@austin.utexas.edu or cbaiz@cm.utexas.edu

Ziareena A. Al-Mualem and Xiaobing Chen contributed equally to this work.

Editor: Valeria Vasquez.

https://doi.org/10.1016/j.bpj.2023.12.019

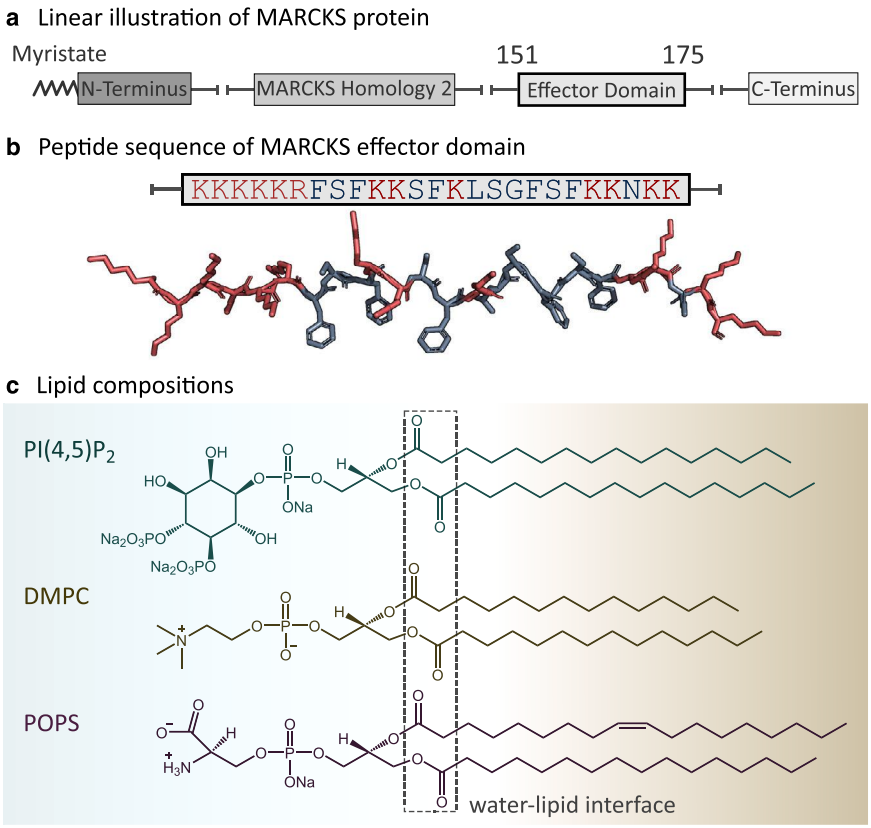

FIGURE 1 Illustration of the MARCKS protein, MARCKS effector domain, and lipids used in this study. (*a*) Linear illustration of MARCKS protein. MARCKS(151–175) indicates the effector domain for membrane binding. (*b*) Peptide sequence of MARCKS effector domain (MARCKS-ED) and the predicted structure in a cartoon representation. Red indicates the positively charged residues. Blue indicates neutral residues. The structure of MARCKS-ED is extracted from the AlphaFold Protein Structure Database with UniProt: F6YSK7. (*c*) Lipid compositions in this study are $PI(4,5)P_2$ (*top*), DMPC (*middle*), and POPS (*bottom*). The dashed gray box indicates the carbonyl groups used as vibrational probes at the water-lipid interface. To see this figure in color, go online.

phosphorylation of serine residues in the MARCKS-ED, which partially neutralizes its electrostatic interaction with the membrane, shifting the equilibrium of full-length MARCKS to a dissociated state. Moreover, the MARCKS-ED fragment is known to interact with calmodulin in a calcium-dependent manner as well as actin. Therefore, the dissociation of MARCKS from the membrane is favored when the serine residues of MARCKS are phosphorylated or when MARCKS-ED forms an alternately bound state with proteins or ions. Although MARCKS switches between membrane-associated and -dissociated states, the biological relevance of this state change remains unclear (13).

Studies of the interaction between reconstituted lipid bilayers and the MARCKS-ED fragment showed that heterogeneous mixtures of lipids undergo domain separation in the presence of the MARCKS-ED (14). Particular emphasis is placed on the action of multivalent basic ligands to form domains enriched in acidic phospholipids, which would dissipate at higher concentrations of the basic ligand (15). Moreover, mixtures that include phosphatidylinositol 4,5-bisphosphate (PIP_2) with phosphatidylserine (PS) also separated in a MARCKS-ED-dependent manner, recruiting PIP_2 to the acidic PS compartments (16). Therefore, the negatively charged lipid domains serve as landing sites for the MARCKS-ED, where the interactions between charged lipids determine the binding activities of MARCKS protein. Nevertheless, it remains an open question as to how a heterogeneous composition of lipids, including different anionic lipids, provides context to the direct interaction between, for example, PIP_2 and MARCKS-ED. It is known that cells modulate both PIP_2 and PS for cell signaling purposes, and therefore we believe that interrogating the biophysical mechanisms of this complex interaction between peptide, PS, and PIP_2 would inform our understanding of the biological importance ascribed to the individual components.

It is important to characterize the local interactions among the protein, lipid, and water molecules at the lipid-water interface to understand the binding mechanism of the MARCKS protein and the roles of PIP_2 and PS lipids. When the MARCKS-ED binds to the lipid membrane, it influences its local environment at the interface and neighboring lipids. By modifying the membrane composition with PIP_2 or PS, we assess the contribution of these negatively charged lipids. In this study, we utilized two-dimensional infrared (2D IR) spectroscopy to investigate the local environment of the lipids when bound to the peptide. 2D IR spectroscopy is a label-free technique that is highly effective in probing the local environments of lipids, allowing us to discern small differences in different lipid compositions. The ester carbonyl stretch of the lipids serves as an excellent indicator of the molecular structure and dynamics at the lipid-water interface. The interfacial environment is sensitive to the lipid composition and distribution within

the membranes. Furthermore, studying water fluctuations at the interface provides a dynamic view of the binding surface that is responsible for ion exchange, protein binding, and proton transfer. Additionally, we employed fluorescence anisotropy to observe the change in rotational diffusion of the fluorophore-tagged MARCKS-ED domain as a measure of peptide binding to lipid vesicles, both with and without the anionic lipids PIP_2 and PS. In brief, changes resulting from alterations in lipid composition highlight the significant roles of anionic lipids in MARCKS-binding events. The study also provides evidence of nonadditive interactions between PIP_2 and PS in MARCKS-ED binding, where they are colocalized both in the presence and absence of peptide.

MATERIALS AND METHODS

Sample preparation

The MARCKS(151–175) sequence is acetyl-KKKKKRFSFKKSFKLSGF SFKKNKK-amide and will be referred to as MARCKS-ED in this article. MARCKS-ED was custom synthesized (>90%; Biomatik, Cambridge, ON, Canada) and lyophilized in 1% v/v DCl/D_2O solution to remove residual trifluoroacetic acid from synthesis. Lipid samples were prepared with 0–1 mol % 1-palmitoyl-2-oleoyl-sn-glycero-3-phospho-L-serine (POPS) sodium salt (>99%; Avanti Polar Lipids, Alabaster, AL, USA), 0–1 mol % D-*myo*-PIP_2 diC16 sodium salt (>95%; Echelon Biosciences, Salt Lake City, UT, USA), with the remaining lipid being 1,2-dimyristoyl-sn-glycero-3-phosphocholine (DMPC) (>99%, Avanti Polar Lipids), as shown in Table 1. The final lipid and peptide concentrations were 50 and 1 mM (2 mol%), respectively, for IR measurements. We selected DMPC as the main bulk lipid to allow us to investigate the effects of headgroups before and after MARCKS-ED binding without any interference from unsaturated tails. Additionally, given that DMPC and POPS have similar phase-transition temperatures around room temperature, we were able to conduct experiments without the issue of overheating the samples, thereby preventing degradation of MARCKS-ED and PIP_2. Note that we intentionally maintained both acidic lipids at 1 mol % to differentiate the effects of PS and PIP_2 on peptide binding. By preserving an equivalent ratio of PS and PIP_2, we can isolate the influence of these lipids on peptide binding and compare the binding results when the peptide has an equal probability of accessing both lipids. The choice of PIP_2 with a 16-carbon tail, which roughly matches the tail lengths of DMPC and POPS, minimizes hydrophobic mismatch and deformation of the lipid bilayer. All chemicals were used as received without further purification.

The lipids, dissolved in chloroform, were dried under a flow of N_2 gas for 2 h and then kept under vacuum for 1 h. The dried lipid films were reconstituted in a 100 mM 3-(N-morpholino)propanesulfonic acid (MOPS) buffer in D_2O (99.8%; Acros Organics, Geel, Belgium), adjusted to pH 7.0 with NaOD. The samples were vortexed and then sonicated at 35°C for 15 min. For IR experiments, MARCKS-ED was added to the samples before vesicle formation to ensure that the lipid interactions are present across both inner and outer leaflets of the vesicle. The samples were vortexed and then sonicated at 35°C for 15 min. To homogenize the samples, the samples underwent 10 freeze-thaw cycles and then were extruded with 40 passes through a 100-nm pore membrane. The samples were left to equilibrate at room temperature for 10 min prior to measurements.

TABLE 1 List of membrane compositions analyzed using 2D IR spectroscopy

Sample no.	Lipid composition in molar ratio	Lipid/MARCKS molar ratio
1	DMPC	no MARCKS
2	DMPC	50:1
3	DMPC/POPS (99:1)	no MARCKS
4	DMPC/POPS (99:1)	50:1
5	DMPC/PIP_2 (99:1)	no MARCKS
6	DMPC/PIP_2 (99:1)	50:1
7	DMPC/PIP_2/POPS (98:1:1)	no MARCKS
8	DMPC/PIP_2/POPS (98:1:1)	50:1

Fluorescence anisotropy

The MARCKS-ED peptide used in fluorescence experiments was tagged with a cyanine 5 (Cy5) dye at the N-terminus. The fluorophore-tagged MARCKS-ED (151–175) sequence is Cy5-KKKKKRFSFKKSFKLSGFSFKKNKK-amide, which will be referred to as MARCKS-ED-Cy5 for simplicity. The custom-synthesized tagged peptide (>90%; Bio-Synthesis, Lewisville, TX, USA) was lyophilized to remove residual trifluoroacetic acid from synthesis. A buffer solution of 100 mM MOPS with 50 mM NaCl was made in Milli-Q water and then titrated to pH 7 using NaOH. 50 mM DMPC, 0.5 mM PIP_2, and 0.5 mM POPS stock solutions in the MOPS/NaCl buffer were made separately and were sonicated at 35°C for 20 min. Appropriate volumes of lipid stock solutions were mixed to make initial solutions of DMPC, DMPC/POPS, DMPC/PIP_2, and DMPC/POPS/PIP_2 to achieve desirable concentrations of 5 mM, 50 μM, and 50 μM for DMPC, POPS, and PIP_2, respectively. Initial samples were vortexed and then sonicated at 35°C for 15 min, followed by 4 freeze-thaw cycles, and were extruded with 40 passes through a 100-nm pore membrane. The initial lipid solutions were then diluted to lower concentrations with the MOPS/NaCl buffer. Appropriate volumes of MARCKS-ED-Cy5 were added after vesicle formation to obtain the final concentration of 40 nM, and 400 μL sample was loaded immediately into quartz cuvettes (Aireka Cells, North Point, Hong Kong, China) before the fluorescence anisotropy measurement. Measurements were performed using a FluoroMax (Horiba, Kyoto, Japan) with the excitation monochromator at 640 nm, the emission monochromator at 660 nm, and both slits at 5 nm. All measurements were taken at room temperature.

IR spectroscopy

2D IR spectroscopy

The lipid ester carbonyl groups serve as sensitive vibrational probes at the lipid-water interface. 2D IR spectra of the ester carbonyl stretching vibrational mode were collected using a custom-built spectrometer described in detail elsewhere (17). Coherence times (t_1) were scanned from 0 to 4 ps in steps of 20 fs. The waiting times (t_2) between the pump and probe pulses were select values from 150 fs to 5 ps. Spectra were collected with phase cycling at a perpendicular pump-probe polarization to reduce residual scatter, and data were collected with a rotating-frame frequency of 1400 cm^{-1}. Each spectrum was produced using 500,000 laser shots (~8 min), and the averaging was doubled for the spectra collected at t_2 values greater than 2 ps to compensate for the decrease in signal to noise from population relaxation. 2D IR spectra were measured at 35°C and under a purge of dry air.

Pump slice amplitude (PSA) analysis

The PSA method is used to compute linear spectra from 2D IR spectra that are more comparable to Fourier transform IR (FTIR) spectra than diagonal slices of 2D IR spectra (18). In brief, PSAs represent the differences between the maxima of positive peaks and the minima of negative peaks of pump slices, which are a series of cuts across the probe axis at constant pump frequencies. PSAs of the 2D IR spectra collected at 150 fs are fitted to two Gaussian functions to estimate hydrogen-bonding populations.

Center line slope (CLS) analysis

Time-dependent 2D IR spectra can elucidate the dynamics of the local environment at the lipid-water interface. 2D lineshapes change over increasing waiting times as a result of the frequency fluctuations of the ester carbonyl stretching mode, and these changes report on the evolution of the frequency-frequency correlation function (FFCF) of the carbonyl. Here, we use the CLS analysis to extract the interfacial dynamics of lipid vesicles (19). In CLS, slices are taken along the probe axis at constant pump frequencies to find the maxima of the positive peak in the 2D IR spectrum. The CLS is calculated from the slope of the best-fit line connecting the peak maxima. Each CLS is fitted with a single exponential decay with an offset. Details of the fitting formula and parameters are given in section S6 of the supporting material. Comparing the exponential fitting parameters among lipid samples with different compositions offers insights into the effects of anionic lipids and MARCKS on the interfacial dynamics of lipid vesicles.

RESULTS

Composition-dependent binding of MARCKS-ED

The change in rotational diffusion of the tagged peptide MARCKS-ED-Cy5 was probed with increasing lipid vesicle concentrations by fluorescence anisotropy. The results are shown in Fig. 2, with the MARCKS-ED-Cy5 peptide anisotropy in 50%, 80%, and 90% glycerol solutions shown as a reference to give the range of values as viscosity of the solution increases. The anisotropy measurement for MARCKS-ED-Cy5 in 90% glycerol solution provides an estimate for a near-maximal anisotropy value of 0.37, which is slightly below the theoretical limit of 0.4. In pure DMPC vesicles, the anisotropy increases noticeably from ~0.2 to ~0.25 in the range of 1250–5000 μM. At the highest lipid concentration (5000 μM), the anisotropy of MARCKS-ED-Cy5 is comparable to that in 50% glycerol. With the inclusion of 1% PIP_2, the anisotropy increases steeply after 625 μM, reaching ~0.45 at a lipid concentration of 5000 μM, higher

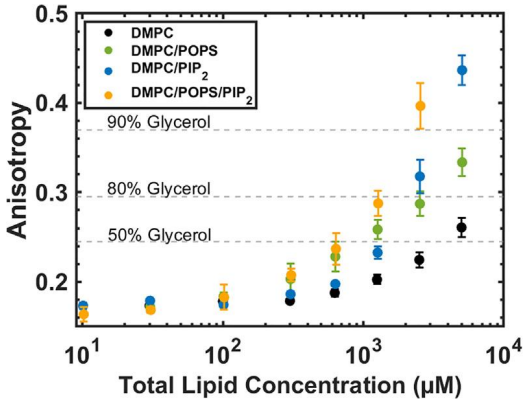

FIGURE 2 Anisotropy of MARCKS-ED-Cy5 as a function of total lipid concentration for 100% DMPC (*black*), 99% DMPC and 1% PIP_2 (*blue*), 99% DMPC and 1% POPS (*green*), and 98% DMPC, 1% POPS, and 1% PIP_2 (*yellow/orange*) at room temperature. The error bars indicate standard deviation. The anisotropy of MARCKS-ED-Cy5 in 50%, 80%, and 90% glycerol in water is shown as a reference with dashed horizontal gray lines. To see this figure in color, go online.

than that of MARCKS-ED-Cy5 in 90% glycerol. The higher-than-anticipated anisotropy measurement beyond the theoretical limit of 0.4 may be attributed to an unexpected interaction between the Cy5 dye and the lipid environment. We anticipate that the increasing lipid concentration saturates binding of the MARCKS-ED-Cy5. However, the ratio of MARCKS-ED-Cy5 to each vesicle also decreases with increasing lipid concentration, and at 40 nM, we estimate that 1 MARCKS-ED-Cy5 molecule binds to each vesicle in 5000 μM lipid solution (see Table S1). To test whether >0.4 anisotropy in our MARCKS-ED-Cy5 and 1% PIP_2 vesicles is a consequence of the low ratio between peptide and vesicle concentrations, we spiked a 40 nM MARCKS-ED-Cy5 in 5000 μM 1% PIP_2 sample up to 200 and 400 nM with unlabeled MARCKS-ED. The anisotropy readings in our sample dropped from 0.48 to 0.41 and 0.39, respectively, in response to the addition of unlabeled peptide (Table S1). Clearly, the Cy5 probe is sensitive to the changes occurring in the 1% PIP2 lipid environment as more peptide molecules interact with each vesicle. With 1% PS, the anisotropy also increases sharply after 300 μM, and rises to 0.33 in the 5000 μM lipid solution, which is greater than in 80% glycerol. The role of PS in the peptide binding to PIP_2 is further investigated by measuring the peptide anisotropy in the presence of both 1% PIP_2 and 1% PS. As previously observed with the 1% PS solution, the anisotropy increases sharply after 300 μM lipid concentration, and the final measurement of ~0.4 is recorded at 2500 μM. We did not attempt to measure a higher concentration of PC/PS/PIP_2 than 2500 mM since the nominal range for anisotropy is <0.4. Interpretation of a higher value than 0.4 would necessitate evaluation of the MARCKS-ED/liposome anisotropy signal as a complex function of binding and higher-order photo-selectivity terms, which is beyond the scope of this work. Note that preparation of lipid samples is also limited at 5000 μM because of an artifactual anisotropy component introduced by scattering at higher concentrations of lipids in liposomal solutions. Based on the anisotropy responses obtained in our different lipid samples, we surmised that liposomal solutions containing 50 mM lipid, regardless of composition, would bind a significant fraction of the 1 mM peptide in subsequent IR experiments.

Interfacial hydration of lipid vesicles with bound MARCKS-ED

The secondary structure of MARCKS-ED bound to lipid vesicles is investigated through circular dichroism (CD) spectroscopy, as detailed in section S2 of the supporting material. The CD spectra are provided in Fig. S1. While an obvious increase in CD peak intensity is observed after peptide binding, indicative of enhanced peptide rigidity, the similar peak shape suggests that the peptide's secondary structure remains mostly random before and after binding to lipid vesicles. It is worth noting that upon binding to

PIP_2, there is a slight trend toward increased structural ordering in MARCKS-ED based on the observations in the CD spectra (see section S2 of the supporting material). Nevertheless, due to the peptide's weak signal and the substantial scattering from lipid vesicles, the baseline of the CD spectra becomes distorted, preventing us from drawing definitive conclusions regarding the changes in MARCKS-ED's secondary structure before and after lipid binding. In short, the structure of MARCKS-ED largely retains its disordered nature, with the possibility of increased ordering when binding to PIP_2 lipids.

FTIR experiments are conducted prior to 2D IR to ensure proper absorbance of the carbonyl peaks and to examine the ordering of lipid tails. Room temperature FTIR spectra of lipid vesicles in the absence or presence of MARCKS-ED are presented in section S3 of the supporting material. Lipid ester carbonyl stretch and CH_2 stretch spectra are included in Figs. S2 and S3, respectively. The absorbance of the lipid ester carbonyl is maintained at ~0.15 OD. The position of the C-H stretch peak is slightly altered by MARCKS-ED binding, indicating different acyl chain ordering. The center frequencies of the symmetric and asymmetric CH_2 stretch peaks, which show the same changes before and after the addition of peptide, are summarized in Table S2. In samples of 100% PC and 1% PIP_2/99% PC vesicles, the acyl chains appear more disordered after peptide binding, as indicated by the blueshift of symmetric and asymmetric stretches by 1–2 cm^{-1}. Such observation is in line with previous work where phosphatidylinositol is found to induce packing defects in PC model membranes (20). However, they become more ordered in the sample with 1% PIP_2/1% PS/98% PC vesicles, as evidenced by the redshifts in the stretches by 1–2 cm^{-1}. It is also worth noting that the blueshift in frequencies of CH_2 stretching modes by 1–2 cm^{-1} is equivalent to the tail order change induced by a temperature increase of >20°C (21).

The interfacial environments are characterized using 2D IR spectroscopy of the lipid ester carbonyl stretching mode, and comparisons are made across eight samples with different lipid compositions (see Table 1). Example 2D IR spectra of the carbonyl stretch for the 100% PC sample with 2% MARCKS-ED are shown in Fig. 3. A broad and asymmetric peak from the ester carbonyl stretches spans the range ~1710 to ~1760 cm^{-1} across all samples. Additional spectra for all samples can be found in section S5 of the supporting material (Figs. S6–S13).

PSAs were calculated from 2D IR spectra of the carbonyl stretch region to further investigate the local environment of the lipid-water interface. Since 2D IR spectroscopy offers background-free spectra and greater sensitivity to changes in lineshapes, comparing PSAs among different lipid compositions can help quantify differences in the interfacial structure. For example, in Fig. 4 *a*, the PSA spectrum of PC exhibits a broad linewidth (~30 cm^{-1}) containing two partially overlapping peaks, which arise from two species

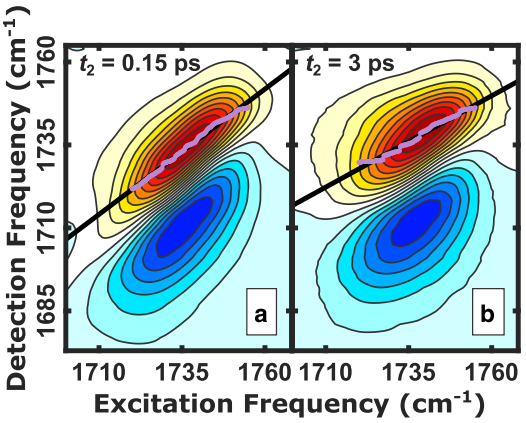

FIGURE 3 Representative 2D IR spectra of lipid carbonyl stretch in the 100% PC sample with 2% MARCKS-ED at waiting times (t_2) of (*a*) 0.15 and (*b*) 3 ps. The purple points represent the points of maximum absorbance at each excitation frequency within a constrained frequency range. The black line is the line of best linear fit of the purple points, which gives the slope for CLS analysis. To see this figure in color, go online.

of ester carbonyl stretches. The peak attributed to the nonhydrogen-bonded species, or 0 HB, appears at ~1747 cm^{-1}, while the singly HB species, or 1 HB, is redshifted to ~1733 cm^{-1}. This observation aligns with previous IR studies of lipid-water interfaces (22–25). The PSAs of the 2D IR spectra at a waiting time of 150 fs were fit with two Gaussian profiles to extract interfacial HB populations (Fig. 4 *a*). Fitting details are provided in section S4 of the supporting material. Additional PSA spectra are presented in Fig. S4. The parameters, along with error bars from Gaussian fittings of PSAs, are depicted in Fig. S5. HB populations can be estimated from peak areas. The calculated populations are consistent regardless of the sample composition: ~88% 1 HB peak and ~12% 0 HB peak. According to the Beer-Lambert law, the area ratio of 1 HB to 0 HB is directly proportional to the HB populations (23). Since the ratio of molar absorptivity of 1 HB to 0 HB was previously determined to be 1.49 (23), the average HB number per ester group can be computed (Fig. 4 *b*). For instance, the HB number for pure PC is approximately 0.8 per ester group, which can also be interpreted as an 80% probability of binding to solvent molecules.

HB dynamics at the lipid-water interface

The time-dependent 2D IR spectra measures the dynamics in the local environments of lipid ester groups. Fig. 3 exhibits the spectra of 100% PC sample with 2% MARCKS-ED at 0.15 and 3 ps. At early waiting times, the peaks appear elongated along the diagonal, where the excitation and detection frequencies are equal, indicating a high correlation between the excitation and detection frequencies. As time progresses, the peaks become rounder, indicating a gradual loss of excitation-detection correlation. The evolution of

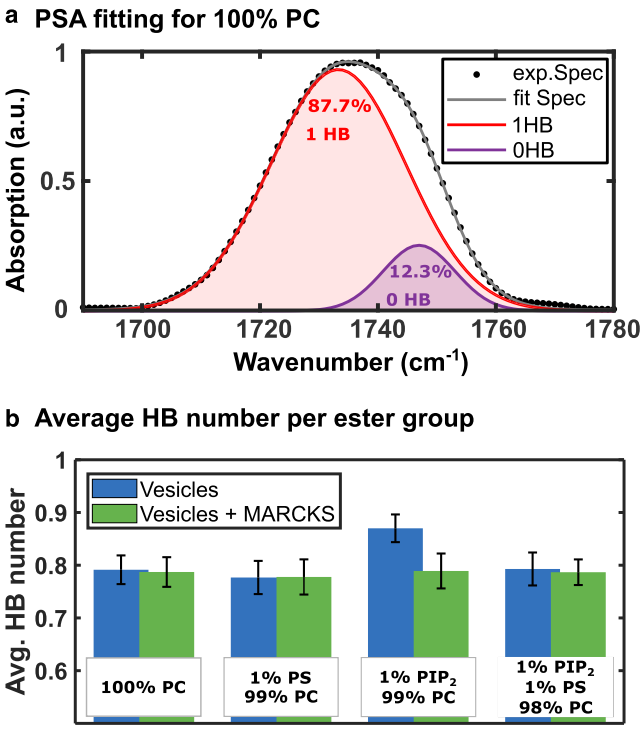

FIGURE 4 Example PSA spectrum and hydrogen-bond populations estimated from Gaussian fits. (*a*) PSA for 100% PC at a waiting time of 150 fs fitted with two Gaussian profiles. Red and purple represent carbonyls hydrogen-bonded with one water (1 HB) and nonhydrogen-bonded (0 HB), respectively. The black dots represent the experimental data, and the gray line is the overall fit. (*b*) Average hydrogen-bond number per ester group estimated from the areas of the Gaussian peaks for the vesicle samples without MARCKS-ED (*blue bars*) and with MARCKS-ED (*green bars*). The error bars are calculated from uncertainties in the fit parameters. Details are provided in Fig. S5. To see this figure in color, go online.

the 2D lineshapes, also known as spectral diffusion, reflects the FFCF of the ester carbonyl stretches (19,26,27), which arises from the rapid fluctuations in the interfacial environment of the ester groups. Fig. 5 shows a comparison of the CLS decays across all measured samples.

All CLS curves start from a value of ~0.8 and decay to ~0.5 within a waiting time of 5 ps, as shown in Fig. 5. The decay amplitude (A) is linked to the amplitude of frequency fluctuation, the offset (y_0) represents the static inhomogeneity of unexplored dynamical processes outside the 5 ps detection window, and τ signifies the relaxation time of the water network fluctuating around the carbonyls. The extracted decay amplitudes and static inhomogeneities are approximately 0.25 and 0.55, respectively, and were consistent across all samples. Results of CLS fitting terms are summarized in Table S3 in section S6 of the supporting material. For the 100% PC samples, the extracted relaxation times are statistically the same for both the vesicles-only and vesicles-with-MARCKS-ED samples, measuring at 1.09 ± 0.04 and 1.10 ± 0.06 ps, respectively. The 1% PS samples exhibited an overall slowdown in dynamics compared to the 100% PC samples and displayed similar dynamics upon the addition of the peptide, ranging from 1.39 ± 0.04 to 1.49 ± 0.07 ps. Interestingly, the 1% PIP_2 sample demonstrated an acceleration in dynamics from 1.55 ± 0.08 to 1.00 ± 0.05 ps with the addition of the MARCKS-ED. Samples containing both 1% PS and 1% PIP_2 showed relaxation times comparable to the 100% PC samples, measuring at 1.00 ± 0.06 ps without the peptide and at 1.07 ± 0.06 ps with the peptide, showing essentially no change.

DISCUSSION

PIP_2 and PS facilitate peptide binding to lipid vesicles

The binding affinity of MARCKS-ED is influenced by membrane composition. MARCKS-ED is basic, with 13 positively charged residues, which implies that MARCKS-ED should interact primarily with the anionic headgroups of PIP_2 and PS. PIP_2 is known to be an important minor lipid species that serves as binding sites for MARCKS-ED (16,28–30). The monovalent acidic lipid, PS, can also increase the affinity between peptide and lipids via nonspecific electrostatic interactions (15,31). The peptide-lipid interactions can be probed through the anisotropy measurement of MARCKS-ED-Cy5. When the peptide is attached to the surface of the lipid vesicle, the peptide configurational space becomes more restricted than in the bulk. With higher lipid concentration or higher binding affinity, the restriction on peptide rotation becomes greater, as evidenced by the increase in the fluorescence anisotropy of MARCKS-ED-Cy5 across all samples in Fig. 2.

Increasing the anionic character of the lipid vesicles by the addition of PIP_2 or PS raises the binding affinity between the peptide and lipid vesicles at higher concentrations (~625 mM), but the anisotropy results are different between PIP_2 and PS, indicating that factors beyond simple electrostatic interactions may factor into MARCKS-ED binding (31). Specifically, the binding affinity is comparable between the PIP_2 and PS samples (perhaps even favoring PS) until a lipid concentration of 300 μM. At higher lipid concentrations, the change in anisotropy becomes steeper with PIP_2, where peptide binding becomes stronger from 1000 to 5000 μM. The steeper character observed in the PIP_2-only vesicle sample also implicates greater cooperativity of interaction between this lipid and the peptide, which suggests a fundamental difference in the mechanism of peptide binding. An intuitive explanation for this is the high charge density of PIP_2 that would energetically disfavor close association of the lipid. However, the multivalent property of PIP_2 has been shown to interact with MARCKS-ED at a 3:1 ratio and exhibit sequestration by the peptide even in the presence of 30% mole fraction PS (32,33). Our data support the prevailing view that MARCKS-ED is capable of selectively sequestering PIP_2 in a lipid environment that is host to a

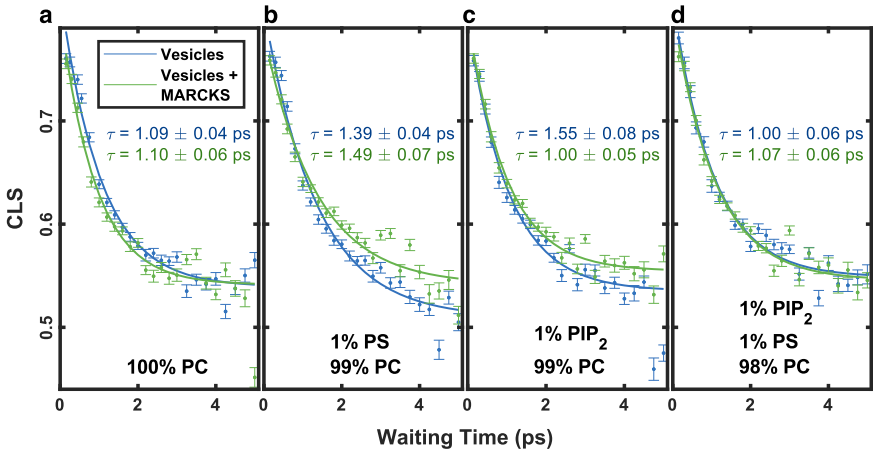

FIGURE 5 Comparison of the CLS decays for the lipid vesicle samples (*blue*) with the addition of MARCKS-ED (*green*) versus waiting time for (*a*) 100% PC, (*b*) 99:1 PC/PS, (*c*) 99:1 PC/PIP_2, and (*d*) 98:1:1 PC/PS/PIP_2. The scattered data points are the slopes of center lines extracted from the 2D IR spectra for different waiting times. The error bars represent standard deviation of the linear fit of center lines. The solid lines are the fitted monoexponential decay curves. To see this figure in color, go online.

high content of anionic lipid, and the validity of a cooperative binding mechanism between PIP_2 and MARCKS-ED appears to be intact. It is important to note that the final PIP_2 anisotropy measurement at a lipid concentration of 5000 μM is distinguished by an anisotropy value outside the nominal range of 0.0–0.4, defined by polarized single-photon excitation of the fluorophore's transition dipole (34). When the anisotropy value exceeds 0.4, it is possible that photo-selection properties have changed for the MARCKS-ED-Cy5 peptide in the samples due to the aggregation of the Cy5 fluorophore. However, the overall contribution of Cy5 aggregates to our measurements should be insignificant since H-aggregates have very low fluorescent yield and J-aggregates have slow kinetics of formation (35,36). Our preferred interpretation of enhanced photo-selectivity for MARCKS-ED in the 1% PIP_2/99% PC vesicle sample is that the peptide fluorophore is sensitive to changes occurring in the lipid environment. A study of fluorescence polarization properties of a probe derived from a 3-hydroxyflavone has shown that photo-selection properties of the probe depended on the local order of the lipid environment (37). In our experiments, the photo-selectivity of the Cy5 probe at a constant concentration of 40 nM may be implicated as follows: as the concentration of lipid increases in our fluorescence anisotropy measurements, the average number of MARCKS-ED-Cy5 molecules per vesicle experiences a gradual decrease to approximately 1 MARCKS-ED per vesicle when the lipid concentration is 5000 μM. We were able to recover nominal anisotropy values that are <0.4 with the addition of unlabeled MARCKS-ED (Table S1). CLS results (Fig. 5 *c*) give compelling evidence that MARCKS-ED alters the lipid phase behavior in the 1% PIP_2/99% PC sample, which agrees with FTIR data, showing increased acyl chain disorder in the presence of MARCKS-ED (Table S2). Fluorescence anisotropy measurements of MARCKS-ED-Cy5 in the 1% PIP_2/99% PC sample would thus measure binding of the peptide with an additional contribution from changes in the lipid environment as the ratio of MARCKS-ED-Cy5 per vesicle shifts.

The presence of PS is hypothesized to enhance the binding of the MARCKS-ED to PIP_2-containing lipid vesicles (30,31,38). In liposome solutions with lipid concentrations exceeding 300 μM, the inclusion of 1% PS alongside 1% PIP_2 facilitates peptide binding to the liposomes compared to PC/PIP_2 sample (Fig. 2). In the literature, it has been demonstrated that MARCKS-ED exhibits a stronger binding affinity for PIP_2 while displaying weaker binding affinity for PS (30,31). Furthermore, MARCKS-ED can sequester multiple PIP_2 in the presence of monovalent acidic lipids such as PS (32). A competition could arise between PIP_2 and PS when both are present within the vesicles. Nevertheless, it is likely that, at lower lipid concentrations, MARCKS-ED favors binding to PS/PIP_2 complexes over PIP_2 alone due to the high charge density among multiple PIP_2 lipids. At this point, PS is shown to indeed facilitate peptide binding to PIP_2-containing vesicles. However, a comprehensive understanding of the lipid interaction mechanism is still pending. Further exploration of the lipid interface is required to unveil the specific roles of these minor lipids in peptide binding.

Lipid-water interfacial hydration remains relatively unchanged

The lipid-water interface is crucial for the localization, organization, and efficient functioning of signaling molecules (26,39,40). It provides a dynamic and interactive environment for membrane communication with proteins, ions, and other small molecules. Investigation of the lipid-water interface with bound peptide is crucial for understanding the interplay between lipid-lipid and lipid-peptide interactions. Though the secondary structure of MARCKS-ED is highly conserved before and after the binding to lipids (30,41), it could potentially change the structure of the lipid bilayer. For example, when MARCKS-ED sequesters PIP_2 lipids, the water molecules surrounding this binding domain are depleted and reorganized to accommodate the 13 positive charges of the MARCKS-ED at the interface. Depending on

the peptide-binding geometry and membrane lipid composition, the interfacial water molecules experience different environments, and the water network ordering is disrupted.

At the lipid interface, water molecules solvate the headgroups of lipids and penetrate the lipid bilayer by ~1 nm down to the ester linkage group (Fig. 1 *c*). The penetration depth or the HB number at the lipid-water interface can be dependent on the lipid compositions, ion concentrations, and other small molecules (23,25,42,43). Interfacial HB populations are estimated from the PSA lineshape (Fig. 4 *a*). A summary of the HB analysis (Fig. 4 *b*) shows that the average number of water molecules solvating the C=O at the interface remained relatively constant, meaning that the addition of MARCKS-ED, PS, or PIP_2 does not make much change in the HB structure at the water-lipid interface. The 1 HB peak width is also wider (Fig. S5), likely due to the larger inhomogeneity in the local environments of bonded species. It is important to note that the 2D IR spectra capture the ensemble average of all the lipid ester carbonyls, meaning that the individual contributions from PC, PIP_2, and PS cannot be evaluated. Thus, the average HB number of 0.8 is an average of all lipid species and indicates the overall penetration of water network.

In samples composed solely of lipids, the negatively charged headgroups of PIP_2 and PS would require a higher number of water molecules for solvation compared to the zwitterionic lipid PC. It is possible that the local environments of PIP_2 and PS experience greater hydration than PC. For example, the 1% PIP_2 sample seems to have slightly higher HB number due to the high negative charges of PIP_2 (Fig. 4). However, the low fraction (1%) of the minor lipid species obscures the distinction of HB populations in the other samples due to the prevailing PC character of the lipid membrane. On the other hand, in samples containing peptides, PIP_2 and PS lipids could become sequestered by MARCKS-ED, resulting in the exclusion of water molecules in the peptide-binding region. Because the effects of peptide binding remain highly localized within these binding domains at the interface, the interfacial structure measured by PSA spectra is primarily influenced by PC lipids, accounting for the unaltered HB number in Fig. 4 *b*.

Interfacial water dynamics is altered by lipid-lipid and lipid-peptide interactions

Lipid membranes engage in a continuous state of dynamic equilibrium with their surroundings. In the current picture, the lipid ester groups primarily form hydrogen bonds with water molecules at the interface (Fig. 4 *b*). The distance and angle between ester carbonyl groups and solvating water molecules fluctuate instantaneously in time. The carbonyl stretches perceive the changes in the solvation geometry, resulting in different electric fields around the ester groups. Such fluctuations in the local environment give rise to the frequency fluctuations of ester carbonyl stretches, observed as the peak shape changes in time-dependent 2D IR spectra (27,44). Time-dependent 2D IR spectra measure the interfacial water fluctuations and provide information on the order of water network, which is sensitive to the lipid-lipid and lipid-peptide interactions. 2D IR has revealed significant changes in interfacial water dynamics in similar systems where the steady-state lineshapes and HB populations are relatively unchanged. For example, Ca^{2+} binding with PS leads to minor changes in the lipid ester carbonyl stretching peak in the FTIR spectrum but significant slowdown in interfacial water dynamics (22). Transmembrane protein crowding also greatly affects interfacial dynamics without changing the HB environment (45).

Interfacial water dynamics are extracted from the time-dependent 2D IR spectra using the CLS method (19). The frequency fluctuation amplitude is found to be relatively comparable for all samples due to the similar water network structure at the lipid-water interface, as evidenced by the similar HB populations in Fig. 4 *b*. The presence of static inhomogeneity could arise from water network reorganization, water rotation, and solvent exchange surrounding the lipid ester carbonyls. The most important information extracted from CLS fitting is the relaxation time of FFCF (τ) in time-dependent 2D IR spectra, which is dominated by the instantaneous angle changes between water and lipid ester carbonyl over time. A summary of the relaxation constants is shown in Fig. 6, exhibiting fluctuation dynamics in the range of 1.0–1.5 ps. Highly ordered water networks or bulk-like water usually make and break hydrogen bonds on the timescale of hundreds of femtoseconds (46). The dynamics is slowed down at the lipid-water interface because the water networks are disrupted by the HB with lipids (26).

The lipid composition and peptide interactions affect the ordering of water network at the interface, which results in

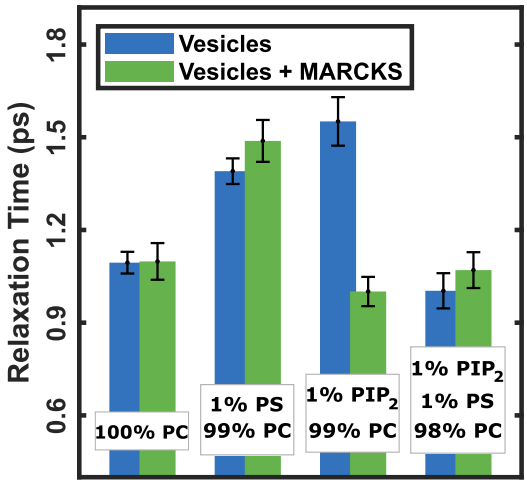

FIGURE 6 Comparison of extracted relaxation times (τ) for the vesicle samples without MARCKS-ED (*blue bars*) and with MARCKS-ED (*green bars*). The black error bars represent the standard deviation of the relaxation time from exponential fittings. To see this figure in color, go online.

different dynamics of HB fluctuations. Among the four vesicle-only samples, the inclusion of 1% PS or 1% PIP_2 resulted in slower dynamics, suggesting a more disordered water network at the interface. This observation aligns with previous research, which established that negatively charged lipid headgroups contribute to a disrupted interfacial water HB networks (22). This phenomenon can be attributed to the difference in headgroup HB and surface potential due to the anionic lipids (47–49). It is worth mentioning that the slight difference between the interfacial dynamics of PC/PIP_2 and PC/PS could be related to the greater negative charge of PIP_2 compared to PS, meaning that PIP_2 requires more solvating water molecules at the interface. As a result, the local water network of PC/PIP_2 is more disrupted, resulting in a less-ordered interfacial water structure and slightly slower interfacial dynamics compared to PC/PS.

The binding of MARCKS-ED peptide in PC/PIP_2 or PC/PS introduces more complexities in interpreting interfacial environments. The inclusion of 1% PS slows down the dynamics regardless of peptide binding, supporting a more disordered interfacial water network, meaning that the peptide does not impact the order of lipid tail packing and interfacial water network. This finding further supports the previously proposed theory that the role of PS in MARCKS-ED binding is solely related to electrostatic interactions. On the contrary, vesicles containing 1% PIP_2 exhibit faster dynamics and thus a more ordered interfacial water network following peptide binding because the nonspecific interactions between MARCKS-ED and PIP_2 induce the reorganization of PIP_2 within the lipid membrane. This observation is in line with prior research on PIP_2 clustering, where the lateral distribution of PIP_2 is shown to be regulated by a variety of membrane-bound proteins (33). Additionally, PIP_2 is sequestered by MARCKS-ED binding even when PS levels reach 30% mol fraction (32,50). Building upon these results, we provide evidence that PIP_2 lipids undergo clustering in the presence of MARCKS-ED.

PIP_2 and PS are colocalized in microdomains of lipid vesicles

Interestingly, when both PIP_2 and PS are present, the interfacial water network becomes more ordered, exhibiting dynamics similar to the 100% PC sample. This contradicts the expectation that negatively charged lipid headgroups would further disrupt the interfacial water network. Our results indicate that the coexistence of PIP_2 and PS in PC vesicles restores the ordering and dynamics of the water network to $\sim$1 ps. These findings highlight the significance of local interactions between PIP_2 and PS, suggesting their partitioning into microdomains within the lipid bilayers. Consequently, the majority of the lipid bilayer, apart from the PIP_2/PS domains, consists primarily of PC, exhibiting an interfacial water network similar to that in pure PC membranes. The fast dynamics observed in PC/PIP_2/PS vesicles suggest that most of the anionic lipids are localized rather than randomly distributed throughout the vesicles, though determining the size and distribution of these specialized PIP_2/PS domains remains challenging.

The binding of MARCKS-ED in PC/PS/PIP_2 does not induce discernable changes in the interfacial water dynamics (Fig. 5). It is highly likely that the presence of both PIP_2 and PS facilitates the formation of specialized regions within lipid bilayers, potentially serving as docking sites for the peptide. Consequently, introducing a peptide at the interface does not cause further changes in the interfacial water network ordering. It is important to note that PS and PIP_2 are unlikely to phase separate into a single large domain or to tightly pack within the same lipid domain. Instead, it is more energetically favorable for them to colocalize into nearby regions, forming multiple microdomains in close proximity. However, the processes of lipid localization are complex and challenging to quantify in terms of domain size and quantity. Therefore, the specific geometric distribution of these microdomains and the number of lipids within them remain unclear at this time. Combining the anisotropy and 2D IR results, we hypothesize that PS alone is unlikely to localize with bound peptides; however, it can enhance the localization of PIP_2 and affect the peptide's binding affinity at the lipid-water interface. Although PIP_2 alone can already localize and bind the peptide with relatively high affinity, its interactions with PS further enhance its effectiveness in binding events. Moreover, the molar ratio of PS in the membrane and its distribution in the inner and outer leaflets could potentially regulate binding events with high specificity in terms of binding positions and capacity. Overall, our implementation of a label-free approach to measure water dynamics at the lipid-water interface, therefore, revealed unexpected properties of the anionic lipids PS and PIP_2. Prior to the addition of MARCKS-ED, we observed colocalization of PS and PIP_2 into microdomains, which is counterintuitive to a purely electrostatic comprehension of the PC/PS/PIP_2 membrane system. Such findings indicate that nonspecific interactions beyond electrostatics, for example, HB among water, lipid, and peptide, are crucial for defining the local environments of lipid membranes. Meanwhile, the measured interfacial water dynamics offers a metric for evaluating the results of molecular dynamics simulations. By quantifying water dynamics at the lipid-water interface, we can establish a connection between simulations and our experiments, thus validating simulated results (22,51).

CONCLUSION

The MARCKS protein, a crucial component of cell signaling, binds to plasma membranes with varying lipid compositions. Its ED can induce domain separation and microdomain formation in lipid vesicles containing PIP_2 and PS. Therefore, these anionic lipids likely play an essential role in the binding

activities of MARCKS. Our findings reveal that both PIP_2 and PS enhance peptide binding to lipid vesicles. Interestingly, their combined presence further facilitates the binding capacity of the MARCKS-ED. While PIP_2 alone localizes to specialized domains and is sequestered by the MARCKS-ED binding, PS remains randomly distributed across membranes before and after MARCKS-ED binding. This suggests that the PS-peptide interaction relies primarily on electrostatic interactions, whereas PIP_2-peptide interactions are more complex. When PS is introduced to PIP_2-containing lipid vesicles, the colocalization of PIP_2 and PS is induced, establishing a microdomain with a dynamic environment for MARCKS-ED binding. In summary, our study provides compelling evidence for the lipid interplay between PIP_2 and PS in the cell signaling pathways involving the MARCKS protein. These results yield molecular insights into potential mechanisms governing cellular functions and potentially offer valuable guidance for advancing biotechnology and drug delivery strategies.

SUPPORTING MATERIAL

Supporting material can be found online at https://doi.org/10.1016/j.bpj.2023.12.019.

AUTHOR CONTRIBUTIONS

Z.A.A.-M., X.C., E.N.S., and C.R.B. conceived and designed the study. Z.A.A.-M. and X.C. conducted and analyzed the data of IR and CD experiments. A.S. and E.N.S. performed the experiments and analysis of fluorescence anisotropy measurements. Z.A.A.-M. and X.C. prepared the main text and supplementary data. A.S. prepared the fluorescence anisotropy figure in the main text. Z.A.A.-M. and X.C. prepared the rest of the figures. All co-authors contributed to editing, commenting on, and revising the manuscript. E.N.S. and C.R.B. acquired funding.

ACKNOWLEDGMENTS

This work was funded by the National Science Foundation (BIO-2129209) and the Welch Foundation (F-1891). Z.A.A.-M. was funded by a Provost Graduate Excellence Fellowship from UT Austin. During the preparation of this work, the authors used ChatGPT-3.5 in order to improve language and readability. After using this tool, the author reviewed and edited the content as needed and take full responsibility for the content of the publication.

DECLARATION OF INTERESTS

The authors declare no competing interests.

REFERENCES

1. Kuhn, M. 2016. Molecular physiology of membrane guanylyl cyclase receptors. *Physiol. Rev.* 96:751–804.
2. Dixon, R. E., and J. S. Trimmer. 2023. Endoplasmic Reticulum-Plasma Membrane Junctions as Sites of Depolarization-Induced Ca2+Signaling in Excitable Cells. *Annual Reviews.* 85:217–243.
3. Urrutia, P. J., and C. González-Billault. 2023. A Role for Second Messengers in Axodendritic Neuronal Polarity. *J. Neurosci.* 43:2037–2052.
4. Yasuda, R., Y. Hayashi, and J. W. Hell. 2022. CaMKII: a central molecular organizer of synaptic plasticity, learning and memory. *Nat. Rev. Neurosci.* 23:666–682.
5. Myat, M. M., S. Anderson, …, A. Aderem. 1997. MARCKS regulates membrane ruffling and cell spreading. *Curr. Biol.* 7:611–614.
6. Brudvig, J. J., J. T. Cain, J. M. Weimer…, 2018. MARCKS regulates neuritogenesis and interacts with a CDC42 signaling network. *Sci. Rep.* 8, 13278.
7. Stumpo, D. J., C. B. Bock, …, P. J. Blackshear. 1995. MARCKS deficiency in mice leads to abnormal brain development and perinatal death. *Proc. Natl. Acad. Sci. USA.* 92:944–948.
8. El Amri, M., U. Fitzgerald, and G. Schlosser. 2018. MARCKS and MARCKS-like proteins in development and regeneration. *J. Biomed. Sci.* 25:43.
9. Chen, Z., W. Zhang, …, M. E. Gershwin. 2021. The myristoylated alanine-rich C-kinase substrates (MARCKS): A membrane-anchored mediator of the cell function. *Autoimmun. Rev.* 20:102942.
10. Peitzsch, R. M., and S. McLaughlin. 1993. Binding of Acylated Peptides and Fatty Acids to Phospholipid Vesicles: Pertinence to Myristoylated Proteins. *Biochemistry.* 32:10436–10443.
11. George, D. J., and P. J. Blackshear. 1992. Membrane association of the myristoylated alanine-rich C kinase substrate (MARCKS) protein appears to involve myristate-dependent binding in the absence of a myristoyl protein receptor. *J. Biol. Chem.* 267:24879–24885.
12. Seykora, J. T., M. M. Myat, …, A. Aderem. 1996. Molecular determinants of the myristoyl-electrostatic switch of MARCKS. *J. Biol. Chem.* 271:18797–18802.
13. Brudvig, J. J., and J. M. Weimer. 2015. X MARCKS the spot: Myristoylated alanine-rich C kinase substrate in neuronal function and disease. *Front. Cell. Neurosci.* 9:165155.
14. Yang, L., and M. Glaser. 1995. Membrane Domains Containing Phosphatidylserine and Substrate Can Be Important for the Activation of Protein Kinase C. *Biochemistry.* 34:1500–1506.
15. Denisov, G., S. Wanaski, …, S. McLaughlin. 1998. Binding of Basic Peptides to Membranes Produces Lateral Domains Enriched in the Acidic Lipids Phosphatidylserine and Phosphatidylinositol 4 , 5-Bisphosphate : An Electrostatic Model and Experimental Results. *Biophys. J.* 74:731–744.
16. Glaser, M., S. Wanaski, …, S. McLaughlin. 1996. Myristoylated alanine-rich C kinase substrate (MARCKS) produces reversible inhibition of phospholipase C by sequestering phosphatidylinositol 4,5-bisphosphate in lateral domains. *J. Biol. Chem.* 271:26187–26193.
17. Edington, S. C., A. Gonzalez, …, C. R. Baiz. 2018. Coordination to lanthanide ions distorts binding site conformation in calmodulin. *Proc. Natl. Acad. Sci. USA.* 115:E3126–E3134.
18. Valentine, M. L., Z. A. Al-Mualem, and C. R. Baiz. 2021. Pump Slice Amplitudes: A Simple and Robust Method for Connecting Two-Dimensional Infrared and Fourier Transform Infrared Spectra. *J. Phys. Chem. A.* 125:6498–6504.
19. Kwak, K., S. Park, …, M. D. Fayer. 2007. Frequency-frequency correlation functions and apodization in two-dimensional infrared vibrational echo spectroscopy: a new approach. *J. Chem. Phys.* 127, 124503.
20. Peng, A., D. S. Pisal, …, S. V. Balu-Iyer. 2012. Phosphatidylinositol induces fluid phase formation and packing defects in phosphatidylcholine model membranes. *Chem. Phys. Lipids.* 165:15–22.
21. Lewis, R. N. A. H., and R. N. McElhaney. 2013. Membrane lipid phase transitions and phase organization studied by Fourier transform infrared spectroscopy. *Biochim. Biophys. Acta.* 1828:2347–2358.
22. Valentine, M. L., A. E. Cardenas, …, C. R. Baiz. 2018. Physiological Calcium Concentrations Slow Dynamics at the Lipid-Water Interface. *Biophys. J.* 115:1541–1551.
23. Valentine, M. L., M. K. Waterland, …, C. R. Baiz. 2021. Interfacial Dynamics in Lipid Membranes: The Effects of Headgroup Structures. *J. Phys. Chem. B.* 125:1343–1350.

24. You, X., E. Lee, …, C. R. Baiz. 2021. Molecular Mechanism of Cell Membrane Protection by Sugars: A Study of Interfacial H-Bond Networks. *J. Phys. Chem. Lett.* 12:9602–9607.
25. Lee, E., X. You, and C. R. Baiz. 2022. Interfacial dynamics in inverted-headgroup lipid membranes. *J. Chem. Phys.* 156, 075102.
26. Flanagan, J. C., M. L. Valentine, and C. R. Baiz. 2020. Ultrafast Dynamics at Lipid–Water Interfaces. *Acc. Chem. Res.* 53:1860–1868.
27. Hamm, P., and M. T. Zanni. 2011. Concepts and Methods of 2D Infrared Spectroscopy. Cambridge University Press, New York.
28. Dietrich, U., P. Krüger, …, J. A. Käs. 2009. Interaction of the MARCKS peptide with PIP2 in phospholipid monolayers. *Biochim. Biophys. Acta.* 1788:1474–1481.
29. Rauch, M. E., C. G. Ferguson, …, D. S. Cafiso. 2002. Myristoylated alanine-rich C kinase substrate (MARCKS) sequesters spin-labeled phosphatidylinositol 4,5-bisphosphate in lipid bilayers. *J. Biol. Chem.* 277:14068–14076.
30. Wang, J., A. Arbuzova, …, S. McLaughlin. 2001. The Effector Domain of Myristoylated Alanine-rich C Kinase Substrate Binds Strongly to Phosphatidylinositol 4,5-Bisphosphate. *J. Biol. Chem.* 276:5012–5019.
31. Arbuzova, A., L. Wang, …, S. McLaughlin. 2000. Membrane binding of peptides containing both basic and aromatic residues Experimental studies with peptides corresponding to the scaffolding region of caveolin and the effector region of MARCKS. *Biochemistry.* 39:10330–10339.
32. Gambhir, A., G. Hangyás-Mihályné, …, S. McLaughlin. 2004. Electrostatic sequestration of PIP2 on phospholipid membranes by basic/aromatic regions of proteins. *Biophys. J.* 86:2188–2207.
33. Wang, J., A. Gambhir, …, S. McLaughlin. 2002. Lateral sequestration of phosphatidylinositol 4,5-bisphosphate by the basic effector domain of myristoylated alanine-rich C kinase substrate is due to nonspecific electrostatic interactions. *J. Biol. Chem.* 277:34401–34412.
34. Gryczynski, I., H. Malak, and J. R. Lakowicz. 1995. Three-photon induced fluorescence of 2,5-diphenyloxazole with a femtosecond Ti:-sapphire laser. *Chem. Phys. Lett.* 245:30–35.
35. Bricks, J. L., Y. L. Slominskii, …, A. P. Demchenko. 2018. Fluorescent J-aggregates of cyanine dyes: basic research and applications review. *Methods Appl. Fluoresc.* 6, 012001.
36. V Berlepsch, H., and C. Böttcher. 2015. H-Aggregates of an Indocyanine Cy5 Dye: Transition from Strong to Weak Molecular Coupling. *J. Phys. Chem. B.* 119:11900–11909.
37. Klymchenko, A. S., S. Oncul, …, Y. Mély. 2009. Visualization of lipid domains in giant unilamellar vesicles using an environment-sensitive membrane probe based on 3-hydroxyflavone. *Biochim. Biophys. Acta.* 1788:495–499.
38. Dietrich, U., P. Krüger, and J. A. Käs. 2011. Structural investigation on the adsorption of the MARCKS peptide on anionic lipid monolayers - Effects beyond electrostatic. *Chem. Phys. Lipids.* 164:266–275.
39. Saha, S., A. Ghosh, …, C. Goswami. 2017. Preferential selection of Arginine at the lipid-water-interface of TRPV1 during vertebrate evolution correlates with its snorkeling behaviour and cholesterol interaction. *Sci. Rep.* 7:16808.
40. Scheidt, H. A., and D. Huster. 2008. The interaction of small molecules with phospholipid membranes studied by 1H NOESY NMR under magic-angle spinning. *Acta Pharmacol. Sin.* 29:35–49.
41. Yan, L., A. J. de Jesus, …, H. Yin. 2015. Curvature Sensing MARCKS-ED Peptides Bind to Membranes in a Stereo-Independent Manner. *J. Pept. Sci.* 21 (7):577–585.
42. Venkatraman, R. K., and C. R. Baiz. 2020. Ultrafast Dynamics at the Lipid–Water Interface: DMSO Modulates H-Bond Lifetimes. *Langmuir.* 36:6502–6511.
43. Tarun, O. B., H. I. Okur, …, S. Roke. 2020. Transient domains of ordered water induced by divalent ions lead to lipid membrane curvature fluctuations. *Commun. Chem.* 3:17.
44. Qin, Z., and D. S. Cafiso. 1996. Membrane Structure of Protein Kinase C and Calmodulin Binding Domain of Myristoylated Alanine Rich C Kinase Substrate Determined by Site-Directed Spin Labeling. *Biochemistry.* 35:2917–2925.
45. Flanagan, J. C., A. E. Cardenas, and C. R. Baiz. 2020. Ultrafast Spectroscopy of Lipid-Water Interfaces: Transmembrane Crowding Drives H-Bond Dynamics. *J. Phys. Chem. Lett.* 11:4093–4098.
46. Perakis, F., L. D. Marco, …, Y. Nagata. 2016. Vibrational Spectroscopy and Dynamics of Water. *Chem. Rev.* 116:7590–7607.
47. Liu, C., Q. Zhong, C. Song…, 2022. Asymmetrical Calcium Ions Induced Stress and Remodeling in Lipid Bilayer Membranes. *Preprint at ChemRxiv.* https://doi.org/10.26434/chemrxiv-2022-24qv4.
48. Kopec, W., A. Żak, …, M. Kepczynski. 2020. Polycation–Anionic Lipid Membrane Interactions. *Langmuir.* 36:12435–12450.
49. Platre, M. P., and Y. Jaillais. 2017. Anionic lipids and the maintenance of membrane electrostatics in eukaryotes. *Plant Signal. Behav.* 12, e1282022.
50. Wen, Y., V. M. Vogt, and G. W. Feigenson. 2021. PI(4,5)P2 Clustering and Its Impact on Biological Functions. *Annu. Rev. Biochem.* 90:681–707.
51. Fathizadeh, A., M. Valentine, …, R. Elber. 2020. Phase Transition in a Heterogeneous Membrane: Atomically Detailed Picture. *J. Phys. Chem. Lett.* 11:5263–5267.